Quantifying the deviation of the tropical upper tropospheric temperature response to surface warming from a moist adiabat

Osamu Miyawaki[1], Zhihong Tan[2], Tiffany A Shaw[1], and Malte Friedrich Jansen[1]

[1]University of Chicago
[2]Princeton University

November 21, 2022

Abstract

Climate models project that tropical warming is amplified aloft in response to increased CO$_2$. Amplification aloft is expected following moist adiabatic adjustment and the Clausius-Clapeyron relation. Here, we show that moist adiabatic adjustment overpredicts the multi-model mean temperature response at 300 hPa by 12.9–25.3\% across the model hierarchy. We show that overprediction is influenced by at least three mechanisms: large-scale circulation, direct effect of CO$_2$, and convective entrainment. Accounting for the large-scale circulation and the direct effect of CO$_2$ reduces overprediction by 5.7\% and 3.8\% respectively, but does not eliminate it. To test the influence of entrainment, we vary the Tokioka parameter in aquaplanet simulations with and without a large-scale circulation. When varying the climatological entrainment rate in the aquaplanet, overprediction varies from 6.7–17.9\%. The sensitivity of overprediction to climatological entrainment rate in the aquaplanet configured in radiative-convective equilibrium agrees well with the predictions of zero-buoyancy bulk-plume models.

Posted on 21 Nov 2022 — CC-BY 4.0 — https://doi.org/10.1002/essoar.10503280.1 — This a preprint and has not been peer reviewed. Data may be preliminary.

Quantifying the deviation of the tropical upper tropospheric temperature response to surface warming from a moist adiabat

Osamu Miyawaki[1], Zhihong Tan[2], Tiffany Shaw[1], Malte Jansen[1]

[1]Department of the Geophysical Sciences, The University of Chicago
[2]Program in Atmospheric and Oceanic Sciences, Princeton University

Key Points:

- Moist adiabatic adjustment overpredicts the tropical upper tropospheric temperature response to warming across the CMIP5 model hierarchy.
- The overprediction is non-zero after accounting for the large-scale circulation and the direct effect of CO_2.
- GFDL AM2.1 aquaplanet simulations show that overprediction scales with climatological entrainment rate.

Corresponding author: Osamu Miyawaki, miyawaki@uchicago.edu

Abstract

Climate models project that tropical warming is amplified aloft in response to increased CO_2. Amplification aloft is expected following moist adiabatic adjustment and the Clausius-Clapeyron relation. Here, we show that moist adiabatic adjustment overpredicts the multi-model mean temperature response at 300 hPa by 12.9–25.3% across the model hierarchy. We show that overprediction is influenced by at least three mechanisms: large-scale circulation, direct effect of CO_2, and convective entrainment. Accounting for the large-scale circulation and the direct effect of CO_2 reduces overprediction by 5.7% and 3.8% respectively, but does not eliminate it. To test the influence of entrainment, we vary the Tokioka parameter in aquaplanet simulations with and without a large-scale circulation. When varying the climatological entrainment rate in the aquaplanet, overprediction varies from 6.7–17.9%. The sensitivity of overprediction to climatological entrainment rate in the aquaplanet configured in radiative-convective equilibrium agrees well with the predictions of zero-buoyancy bulk-plume models.

Plain Language Summary

Climate models project that tropical warming will be amplified in the upper troposphere in response to increased CO_2 concentration. This warming pattern is expected based on the increased release of latent heat in a warmer climate (moist adiabatic adjustment). Understanding the vertical profile of warming has important implications for the strength of convective storms, the subtropical climate through its influence on the large-scale circulation, and the climate sensitivity. Here, we compare the moist adiabatic prediction to the warming response across a hierarchy of climate models. We find that the moist adiabat overpredicts the tropical warming aloft across the model hierarchy. We quantify the influence of three mechanisms that are missing in the moist adiabat: 1) different temperature responses in regions of ascent versus descent, 2) the direct effect of increased CO_2 in the absence of surface temperature increase, and 3) convective entrainment (the mixing of dry environmental air into moist ascent). Accounting for the first two mechanisms reduces the overprediction but does not eliminate it. In idealized aquaplanet simulations, we find that stronger entrainment leads to greater overprediction, in agreement with the expectation based on a simple model for the tropical temperature profile that includes the effect of entrainment.

1 Introduction

One of the earliest general circulation model (GCM) predictions of the response to increased CO_2 is amplified warming aloft in the tropics (Manabe & Wetherald, 1975; Manabe & Stouffer, 1980). This prediction has since been confirmed by observations (Santer et al., 1996; Thorne et al., 2011; Flannaghan et al., 2014) and state-of-the-art models such as coupled Atmosphere-Ocean GCMs (AOGCMs) (Vallis et al., 2015) and cloud resolving models (CRMs) (Lau et al., 1993; Romps, 2011). The tropical temperature response has important implications for the global climate, as it sets the 1) static stability in the tropics, which influences the strength of deep convection (Singh & O'Gorman, 2013; Seeley & Romps, 2015), 2) meridional temperature gradient, which influences the position of the Hadley Cell edge and subtropical jet (Shaw et al., 2016), and 3) lapse rate feedback in the tropics, which exerts a strong influence on the global climate sensitivity owing to the large contribution of the tropics to the global mean (Popke et al., 2013; Po-Chedley et al., 2018).

Amplified tropical upper tropospheric warming in response to increased CO_2 is predicted from the adjustment of a moist adiabat (Held, 1993). In particular, for a 4 K warming at the surface with fixed relative humidity, moist adiabatic adjustment predicts warming aloft of 10 K. While the moist adiabatic prediction is intuitive, it does not consider many other processes that may influence the temperature response to warming, such as the large-scale circulation, the direct effect of CO_2, and convective entrainment.

Emanuel et al. (1994) show that in the presence of a strong large-scale circulation, the free troposphere and the sub-cloud layer become decoupled in regions of climatological descent. Thus, we expect moist adiabatic adjustment to apply only over regions of deep convection. Brown and Bretherton (1997), Flannaghan et al. (2014), and Fueglistaler et al. (2015) use precipitation-weighting to show that observed temperature trends in the upper troposphere are more strongly linked to surface trends in regions of deep convection. Andrews and Webb (2018) further demonstrate the importance of the large-scale circulation on the tropical warming response by showing in the HadGEM2-A model that localized SST warming in the western Pacific (where there is climatological deep convection) results in a warming response with strong amplification aloft, whereas the SST warming in the eastern Pacific (climatological descent) leads to warming confined below the tropical inversion. As Andrews and Webb (2018) focus on the role of the tropical temperature response on the lower-tropospheric stability, they do not quantify the deviation of the temperature response from a moist adiabat.

We do not expect the direct effect of CO_2 to lead to moist adiabatic adjustment because it does not impact the global-mean surface temperature. However, it does impact the large-scale circulation and tropical precipitation response (Bony et al., 2013; Merlis, 2015), and the tropospheric warming due to the direct effect is nearly uniform in height (He & Soden, 2015; Wang & Huang, 2020). Thus, we expect the moist adiabat to overpredict the temperature response in the presence of the direct effect of CO_2.

We expect convective entrainment to weaken the amplification of warming aloft compared to a moist adiabat, as an entraining parcel releases less latent heat. Singh and O'Gorman (2013) and Seeley and Romps (2015) show that the increase in convective available potential energy (CAPE) with warming as obtained from CRMs is consistent with that predicted by the zero-buoyancy bulk-plume model. The zero-buoyancy bulk-plume model is a simple model for the tropical temperature profile that includes the effect of climatological convective entrainment. As CAPE quantifies the deviation of a temperature profile from a moist adiabat, increasing CAPE with warming is consistent with the overprediction of upper tropospheric warming by the moist adiabatic adjustment theory. Although previous studies have implied convective entrainment as an explanation for the overprediction of upper tropospheric warming by the moist adiabat (Tripati et al., 2014; Po-Chedley et al., 2019), the influence of varying entrainment rates on the temperature response in GCMs has not yet been reported in the literature.

Here, we quantify the moist adiabatic prediction in response to warming across the CMIP5 model hierarchy. We show that the moist adiabat overpredicts the modeled temperature response. We quantify the importance of three mechanisms on the overprediction of the moist adiabat: 1) the large-scale circulation, 2) the direct effect of CO_2, and 3) convective entrainment. We quantify the importance of convective entrainment by varying the parameterized entrainment rate in idealized aquaplanet simulations.

2 Methods

2.1 CMIP5 models

We examine the tropical temperature response to warming across the climate model hierarchy using CMIP5 data (Taylor et al., 2012). At the most complex end, we consider the AOGCM response to a quadrupling of CO_2 (abrupt4$\times$$CO_2$) relative to a pre-industrial climate (piControl) in 29 models (Supplementary Table S1). We average the last 30 years of the 150-year simulation to study the near-equilibrium response.

In the mid-range of complexity, we consider 11 atmospheric GCMs (AGCMs, see Supplementary Table S1) that prescribe the sea-surface temperature (SST) according to observations from 1979 to 2008 following the AMIP protocol (Gates, 1992). The indirect effect of CO_2 increase is quantified by imposing: 1) spatially-varying SST warming based on the CMIP3 multi-model mean response (amipF) and 2) uniform SST warming of 4 K (amip4K). This allows us to study the importance of patterned SST warming. We also consider the direct effect of increased CO_2 in the absence of SST changes (amip4$\times$$CO_2$) and we add the direct and indirect effects to get the total response to increased CO_2 (amipF/4K+4$\times$$CO_2$) that can be compared to the AOGCM response. We take the average over the entire 30 years of each simulation.

Finally, at the simple end we consider 9 aquaplanet AGCMs (see Supplementary Table S1). The indirect effect is quantified as a response to a uniform SST warming of 4 K (aqua4K) relative to the aquaplanet configured with the qObs SST profile (aquaControl) (Neale & Hoskins, 2000). We also consider the direct effect of increased CO_2 (aqua4$\times$$CO_2$) and add it to the indirect effect to get the total response to increased CO_2 in the aquaplanet (aqua4K+4$\times$$CO_2$).

2.2 GFDL AM2.1 aquaplanet GCM

In order to understand the importance of entrainment for the tropical temperature response to surface warming we configure the GFDL AM2.1 aquaplanet GCM (hereafter GFDL) with the Relaxed Arakawa-Schubert (RAS) convection scheme (Moorthi & Suarez, 1992). In the RAS scheme, the Tokioka parameter (α) controls the minimum entrainment rate ($\epsilon_{\min}$) as follows:

$$\epsilon_{\min} = \frac{\alpha}{D}\,, \tag{1}$$

where D is the depth of the planetary boundary layer. This constraint only affects plumes that detrain above 500 hPa, thus the Tokioka parameter controls the entrainment rate of deep convection only. Tokioka et al. (1988) varied α to study the influence of convective entrainment on the Madden–Julian oscillation. The default climatological value is $\alpha = 0.025$ in GFDL. To investigate the role of entrainment on the tropical temperature response, we perturb α from its default climatological value as follows: $\alpha = 0$, 0.00625, 0.0125, 0.05, and 0.1.

As varying α only indirectly affects the actual entrainment rate in the model, we quantify the entrainment rate using the output from the RAS scheme. The bulk entrainment rate $\langle\epsilon\rangle$ is then calculated as the entrainment rate vertically averaged from 850–200 hPa. The expectation is that as convective entrainment rate increases (increasing α), the convecting plume becomes more sub-saturated, latent heating decreases, and the temperature response to surface warming weakens in the upper troposphere.

We vary the entrainment in two configurations of the GFDL model: 1) the standard aquaplanet configured with the qObs SST profile (GFDLaqua) (Neale & Hoskins, 2000) and 2) rotating radiative-convective equilibrium (RCE) configured with a spatially uniform SST of 300 K (GFDLrce). The latter allows us to test for the robustness of our results in the absence of a large-scale circulation, which is a common idealized model configuration for the tropics (Wing et al., 2018). For both configurations we investigate the response to a uniform SST warming of 4 K (GFDLaqua4K and GFDLrce4K). Following Tan et al. (2019) the GFDL aquaplanet uses RRTMG radiation and does not include the radiative effects of ozone and clouds.

We compare the tropical temperature response to warming with varying climatological entrainment in the aquaplanet to the zero-buoyancy bulk-plume models of Singh and O'Gorman (2013), hereafter SO13, Romps (2014), hereafter R14, and Romps (2016), hereafter R16. The zero-buoyancy bulk-plume model is a simple 1-D model that includes the effect of convective entrainment in RCE. The SO13 model assumes a fixed environmental relative humidity, while the R14 and R16 models explicitly consider the water vapor budget to predict relative humidity, which is further assumed to be vertically constant in R16. For the SO13 model, we assume a constant relative humidity profile of 80%. For the R14 model, we assume a constant ratio of gross evaporation to gross condensation of 0.75 (α in R14) as this gives a close fit to both the GFDLrce and SO13 results. For the R16 model, we assume a constant precipitation efficiency of 0.25 (PE in R16) to be consistent with the value of gross evaporation to condensation rate chosen for the R14 model. We configure all other parameters using the same values as reported in the literature.

2.3 Calculating the moist adiabat and its overprediction

We calculate the moist adiabatic temperature by setting the initial condition of the rising parcel as the annual mean 2 m temperature, humidity, and surface pressure. For models where the 2 m fields are not available, we interpolate the three dimensional temperature and humidity fields to the surface pressure. Where the surface pressure is greater than the lowest pressure level of the vertical grid (1000 hPa), we linearly extrapolate from the 1000 hPa value.

We integrate the dry adiabatic lapse rate Γ_d up to the lifted condensation level (LCL). During this dry ascent, we assume that the water vapor mixing ratio is conserved. Above the LCL, we calculate temperature by integrating the moist-adiabatic lapse rate Γ_m following the definition in the American Meteorological Society (AMS) glossary (AMS, cited 2020: Moist-adiabatic lapse rate).

$$\Gamma_m = \Gamma_d \frac{1 + \frac{L_v r_v}{RT}}{1 + \frac{L_v^2 r_v}{c_{pd} R_v T^2}} , \tag{2}$$

where L_v is the latent heat of vaporization, r_v is the vapor mixing ratio, R is the specific gas constant of dry air, R_v is the specific gas constant of water vapor, T is temperature, and c_{pd} is the isobaric specific heat capacity of dry air. This moist adiabat is a simplified form of a moist pseudoadiabat where it is assumed that all condensates precipitate out immediately and $r_v \ll 1$. Furthermore, we do not consider the effect of freezing (latent heat of fusion).

We quantify the overprediction O_p of the moist adiabatic response at a pressure level p as follows:

$$O_p = \frac{\Delta T_{m,p} - \Delta T_p}{\Delta T_s} \tag{3}$$

where Δ denotes the difference between the warmer and climatological climates, T_p is the GCM temperature at pressure level p, $T_{m,p}$ is the moist adiabatic temperature at pressure level p, and T_s is the surface temperature. We evaluate overprediction at 300 hPa following Fueglistaler et al. (2015). The tropical-mean overprediction is obtained from horizontally-averaging between 10°S and 10°N.

To test the impact of the large-scale circulation, we average overprediction only over regions of climatological ascent at 500 hPa that exceeds the 75th percentile value in the tropics following Sherwood et al. (2014). This corresponds to ≈ -35 hPa/d in the multi-model mean climatology of the piControl and AMIP simulations. The overprediction in regions of deep convection is then obtained from the horizontally-averaged overprediction within regions that satisfy the 75th percentile pressure velocity criteria. We use -35 hPa/d as the threshold value across all models. We do not filter the GFDLrce response by vertical motion due to the absence of a large-scale circulation.

3 Results

3.1 Overprediction across the CMIP5 model hierarchy

Moist adiabatic warming systematically overpredicts the multi-model mean upper tropospheric warming across the CMIP5 model hierarchy (red bars in boxes Fig. 1a). According to a t-test, the difference in mean overprediction between abrupt4×CO_2 and the simpler models is statistically significant at the 5% level (Supplementary Table S2). The multi-model mean overprediction varies by a factor of 2 across the model hierarchy, from 25.3% for abrupt4×CO_2 to 16.6%, 17.0%, and 12.9% for amipF, amip4K, and aqua4K, respectively. The overprediction is largest in the upper troposphere (Supplementary Fig. S1) and is similar for alternative definitions of moist adiabats, such as the pseudoadiabat and the reversible adiabat (Supplementary Table S3).

In what follows we focus on quantifying the impact of the following mechanisms on overprediction: 1) large-scale circulation, 2) direct effect of CO_2, and 3) convective entrainment.

3.2 Large-scale circulation

The moist adiabatic prediction does not take into account the presence of the large-scale climatological circulation or its response to warming. Since the moist adiabat is a model of a convecting parcel, we expect overprediction to be smallest over regions of deep convection (defined here as regions where climatological $\omega < -35$ hPa/d at 500 hPa).

Overprediction is small in regions of deep convection such as the western Pacific warm pool (Fig. 2a–d, inside the red contour line). Conversely, overprediction is large over the eastern Pacific, which is characterized by climatological descent (Fig. 2a–d, regions outside of red contour line). Overprediction over the eastern Pacific is smaller in amip4K compared to amipFuture, suggesting that enhanced future warming in the eastern Pacific contributes to overprediction. Overprediction is zonally uniform in aqua4K (Fig. 2e) and nearly meridionally uniform as most of 10°N/S is a region of climatological deep convection in the aquaplanet.

When averaged only over regions of deep convection, multi-model mean overprediction decreases to 19.3%, 9.3%, and 13.4% for abrupt4×CO_2, amipF, and amip4K (Fig. 1b). This decrease is statistically significant at the 5% level (Supplementary Table S4). In contrast, the multi-model mean overprediction over regions of deep convection for aqua4K slightly increases to 13.1%, but this increase is not statistically significant. Clearly, the climatological large-scale circulation has an influence on the tropical temperature response, but accounting for this does not eliminate overprediction.

3.3 Direct effect of CO_2

The direct effect of increased CO_2 has a significant impact on the tropical circulation and precipitation but does not lead to significant global-mean surface warming (Bony et al., 2013). When the response to the direct effect of CO_2 is added to the surface warming effect in the AGCM and aquaplanet models, the multi-model mean overprediction over regions of deep convection increases to 20.1%, 21.1%, and 16.6% for amipF, amip4K, and aqua4K, respectively (compare Fig. 1b to Fig. 3), and the AMIP model results become more similar to CMIP5 models. A t-test shows that this increase is statistically significant at the 5% level for all three model configurations (Supplementary Table S5). Thus, the direct effect of CO_2 contributes to a non-zero overprediction as expected from previous work that showed the tropical temperature response to the direct effect of CO_2 is vertically uniform (compare vertical structure of black and orange lines in Supplementary Fig. S2).

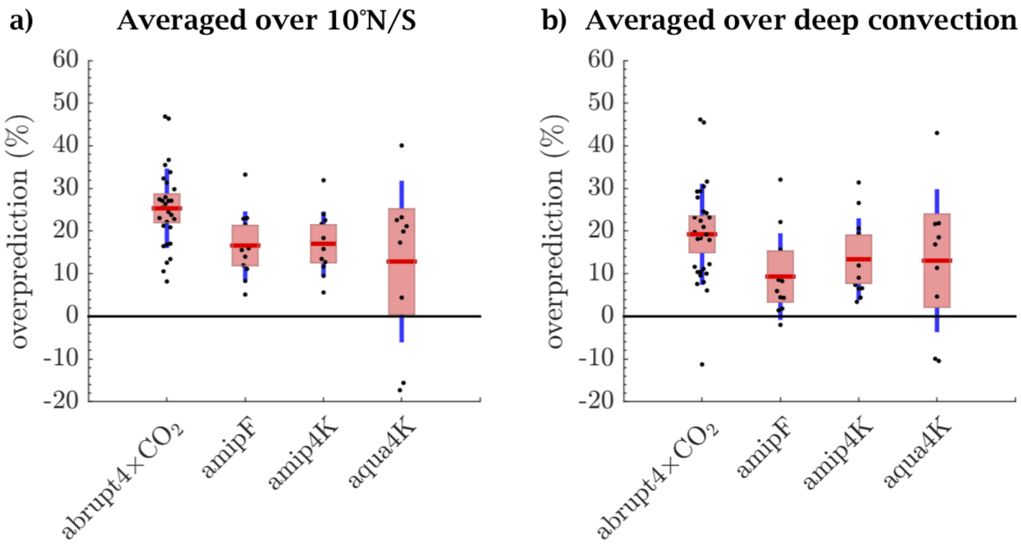

Figure 1. a) Intermodel spread of overprediction across the CMIP5 model hierarchy. For each model configuration, black dots denote overprediction of individual models, the red horizontal line is the mean, the red vertical bar is the 5–95% confidence interval of the mean, and the blue vertical line is the standard deviation. b) Same as a), but overprediction averaged only over regions of deep convection (defined as where $\omega < -35$ hPa/d at 500 hPa).

3.4 Convective entrainment

Even after accounting for the large-scale circulation and the direct effect of CO_2, overprediction is still non-zero (as shown by the AMIP and aquaplanet model results in Fig. 1b). This motivates us to consider the role of entrainment on overprediction, another mechanism that is missing in the moist adiabatic prediction. We study how the strength of climatological entrainment in the RAS convection scheme affects the magnitude of the overprediction in the GFDL model. With the default Tokioka parameter ($\alpha = 0.025$), the moist adiabat overpredicts the GFDLrce4K and GFDLaqua4K response by 11.6% (Supplementary Table S3) and 13.2% (Supplementary Table S6), respectively. The magnitude of overprediction in GFDL is similar to that of the CMIP5 aqua4K multi-model mean, making GFDL a good representative model for this study.

When the Tokioka parameter is increased and thus there is a larger entrainment rate, the temperature response is weakened aloft in both the RCE (Fig. 4a) and aquaplanet (Fig. 4b) configurations. The range of the overprediction obtained from varying the climatological entrainment rate in GFDLrce4K (GFDLaqua4K) is 6.7% to 17.1% (8.3% to 17.9%). Increasing α beyond the range shown here does not further increase the entrainment rate. Thus, the range of bulk entrainment rates obtained here represent nearly the full extent of the entrainment rate regime that can be studied by perturbing the Tokioka parameter in GFDL.

We find that overprediction is strongly correlated with the logarithm of the climatological entrainment rate for both GFDLrce4K ($R = 0.95$, see Fig. 4c) and GFDLaqua4K ($R = 0.98$, see Fig. 4d). While the range of overprediction obtained in GFDLaqua4K is similar to that of GFDLrce4K, GFDLaqua4K exhibits larger entrainment rates given the same Tokioka parameter. The sensitivity of overprediction to the strength of climatological entrainment obtained in GFDLrce4K is consistent with the zero-buoyancy bulk-plume models of SO13 and R14 up to $\langle\epsilon\rangle = 0.1$ km^{-1} (dashed and solid black lines in

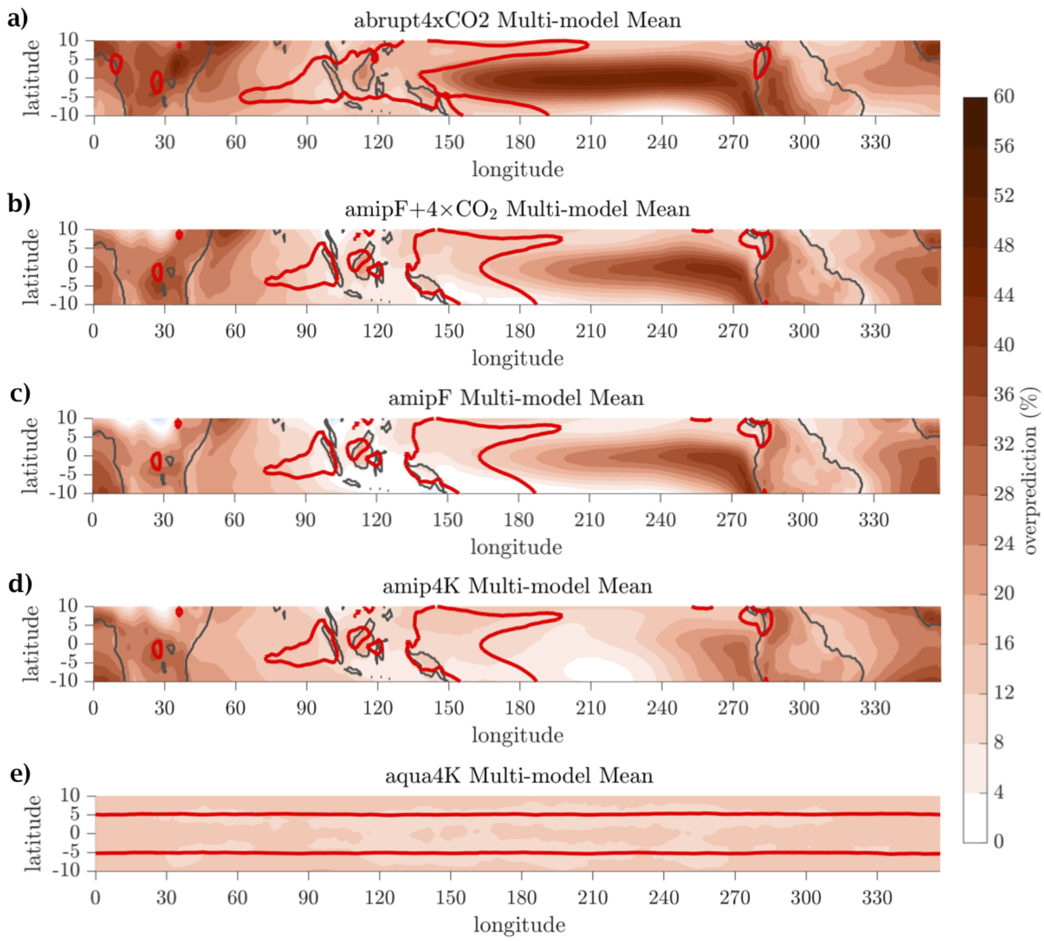

Figure 2. a) Spatial structure of the overprediction of the moist adiabat at 300 hPa in response to warming for the CMIP5 multi-model mean. The red contour denotes the boundary of the multi-model mean climatological deep convection as described in the text. b)–e) are the same for the amipF+4×CO_2, amipF, amip4K, and aqua4K multi-model mean responses, respectively.

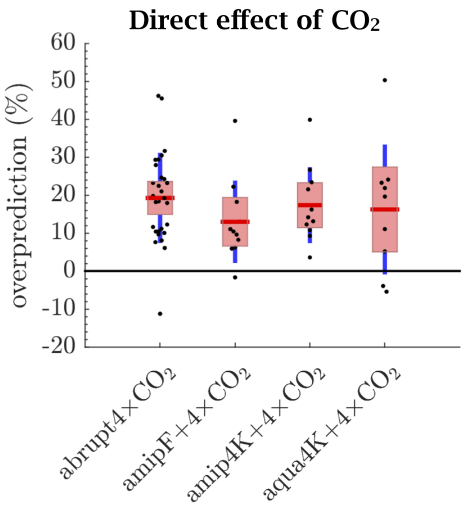

Figure 3. Same as Fig. 1b but including the direct effect of CO_2 in the AMIP and aquaplanet model results.

Fig. 4c). The R16 model predicts weaker overprediction for a given climatological entrainment rate compared to GFDLrce, SO13, and R14. The R16 prediction does not change substantially with varying values of precipitation efficiency.

4 Summary and Discussion

4.1 Summary

Here, we investigate the accuracy of the moist adiabatic prediction of the tropical upper tropospheric temperature response to warming. We found that the moist adiabat overpredicts the multi-model mean tropical upper tropospheric warming at 300 hPa by 12.9–25.3% across the CMIP5 model hierarchy. We quantified the importance of three mechanisms, not included in the moist adiabat theory, to the overprediction: 1) large-scale circulation, 2) direct effect of CO_2, and 3) convective entrainment. The importance of convective entrainment was quantified by varying the Tokioka parameter in idealized aquaplanet simulations. Our conclusions are:

1. The climatological large-scale circulation has a significant impact on overprediction. Overprediction is largest in regions of descent and weak ascent. Overprediction is smaller but non-zero in tropical regions of deep convection. This explains why multi-model mean overprediction is higher for the amip4K response (17.0%) compared to the aqua4K response (12.9%), which does not include climatological descent in the deep tropics (10°N/S).
2. The direct effect of increased CO_2, which impacts tropical circulation and precipitation but not global-mean warming, contributes significantly to overprediction. This explains why multi-model mean overprediction is higher for the abrupt4×CO_2 response (25.3%) compared to the configurations with prescribed surface warming (16.6% for amipF, 17.0% for amip4K, and 12.9% for the aqua4K).
3. Parameterized convective entrainment contributes significantly to overprediction in the GFDL aquaplanet model configured with various Tokioka parameters. Overprediction scales with the logarithm of the climatological entrainment rate in the GFDL model. The sensitivity of overprediction to the climatological entrainment

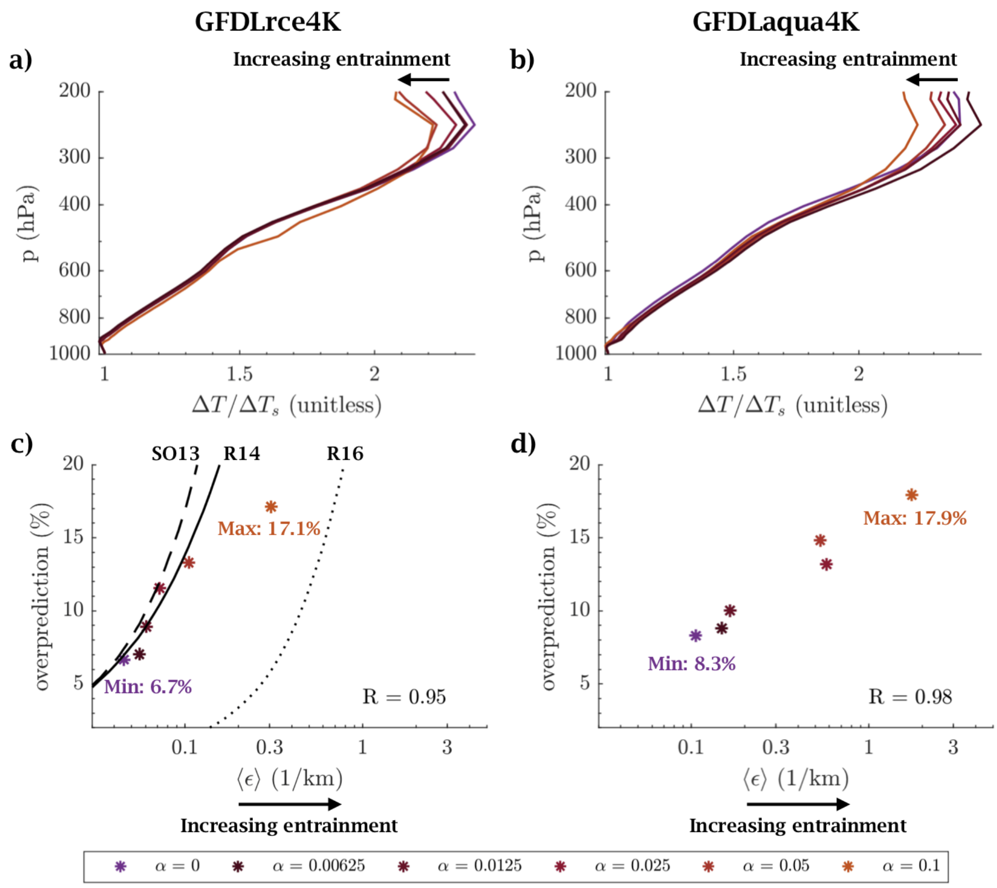

Figure 4. Temperature response in the GFDL aquaplanet when varying the Tokioka parameter for the a) RCE (GFDLrce4K) and b) aquaplanet (GFDLaqua4K) configurations. Overprediction of the moist adiabat increases with the strength of climatological entrainment for c) GFDLrce4K and d) GFDLaqua4K. The deviation as predicted by zero-buoyancy bulk-plume models of Singh and O'Gorman (2013) (labeled SO13), Romps (2014) (labeled R14), and Romps (2016) (labeled R16) are shown as black lines in panel c.

rate in the RCE configuration agrees well with the zero-buoyancy bulk-plume models of Singh and O'Gorman (2013) and Romps (2014). The Romps (2016) model does not agree as closely. This may be due the additional simplifying assumptions that it makes about the vertical structure of entrainment, detrainment, and relative humidity.

4.2 Discussion

While Tripati et al. (2014) and Po-Chedley et al. (2019) attribute the overprediction of the moist adiabat to convective entrainment, our results show that the large-scale circulation and the direct effect of CO_2 also contribute to overprediction. This suggests that the predictions made by the zero-buoyancy bulk-plume models may have limitations outside of the idealized RCE configuration. Indeed, while the sensitivity of overprediction to climatological entrainment in the GFDL RCE aquaplanet agrees well with the zero-buoyancy bulk-plume model, this is not the case for the GFDL aquaplanet with a large-scale circulation. Future work could evaluate the bulk-plume model of Singh et al. (2019), which improves on the Singh and O'Gorman (2013) and Romps (2014) models by also considering the effect of the large-scale vertical motion on the predicted temperature response.

In our study, we perturbed the entrainment rate in an aquaplanet model by an order of magnitude but were not able to capture the full intermodel spread among the aqua4K models. Some possible reasons that our perturbation experiment failed to capture the full spread of overprediction include: 1) the RAS convection scheme is not used by all CMIP5 aquaplanet models and other convection schemes may show greater sensitivity to entrainment, 2) the entrainment response to warming (rather than the climatological entrainment) may influence overprediction, and 3) physical processes other than entrainment may influence overprediction. The importance of 1) may be addressed by running experiments using a different convection scheme that more explicitly allows the entrainment rate to be controlled. The importance of 2) may be quantified by prescribing different entrainment rates in a warmer climate. Prescribing different Tokioka parameters in the control and warm climates of the GFDL aquaplanet leads to a large range of overprediction (-40.4%–73.5%, see Supplementary Fig. S3). However, parameterized entrainment must be compared to more direct measures of entrainment such as those diagnosed from cloud-permitting model simulations (Romps, 2010). Future work could also explore 3) by quantifying the influence of other processes that are not represented in a moist adiabat on overprediction, such as precipitation efficiency, the ice phase, and cloud radiative effects.

This work highlights the limitations of moist adiabatic adjustment as a quantitative theory for the tropical temperature response predicted by climate models, and provides a first step towards a mechanistic understanding of this misfit. A full understanding of tropical lapse rate changes is critical to determine the robustness of model predictions, and to provide confidence in tropical climate forecasts more generally.

Acknowledgments
We acknowledge the University of Chicago Research Computing Center for providing the computational resources used to carry out this work. TAS acknowledges support from NSF (AGS-1742944). Data supporting the conclusions are available through Knowledge@UChicago: `http://knowledge.uchicago.edu/record/2204?&ln=en`.

References

AMS. (cited 2020: Moist-adiabatic lapse rate). *Glossary of meteorology.* ([Available online at `http://glossary.ametsoc.org/wiki/Moist-adiabatic_lapse`

_rate])
Andrews, T., & Webb, M. J. (2018). The dependence of global cloud and lapse rate feedbacks on the spatial structure of tropical pacific warming. *Journal of Climate*, *31*(2), 641–654. doi: https://doi.org/10.1175/JCLI-D-17-0087.1

Bony, S., Bellon, G., Klocke, D., Sherwood, S., Fermepin, S., & Denvil, S. (2013). Robust direct effect of carbon dioxide on tropical circulation and regional precipitation. *Nature Geoscience*, *6*(6), 447–451. doi: https://doi.org/10.1038/ngeo1799

Brown, R. G., & Bretherton, C. S. (1997). A test of the strict quasi-equilibrium theory on long time and space scales. *Journal of the atmospheric sciences*, *54*(5), 624–638. doi: https://doi.org/10.1175/1520-0469(1997)054⟨0624:ATOTSQ⟩2.0.CO;2

Emanuel, K. A., David Neelin, J., & Bretherton, C. S. (1994). On large-scale circulations in convecting atmospheres. *Quarterly Journal of the Royal Meteorological Society*, *120*(519), 1111–1143. doi: https://doi.org/10.1002/qj.49712051902

Flannaghan, T., Fueglistaler, S., Held, I. M., Po-Chedley, S., Wyman, B., & Zhao, M. (2014). Tropical temperature trends in atmospheric general circulation model simulations and the impact of uncertainties in observed ssts. *Journal of Geophysical Research: Atmospheres*, *119*(23), 13–327. doi: https://doi.org/10.1002/2014JD022365

Fueglistaler, S., Radley, C., & Held, I. M. (2015). The distribution of precipitation and the spread in tropical upper tropospheric temperature trends in cmip5/amip simulations. *Geophysical Research Letters*, *42*(14), 6000–6007. doi: https://doi.org/10.1002/2015GL064966

Gates, W. L. (1992). An ams continuing series: Global change–amip: The atmospheric model intercomparison project. *Bulletin of the American Meteorological Society*, *73*(12), 1962–1970. doi: https://doi.org/10.1175/1520-0477(1992)073⟨1962:ATAMIP⟩2.0.CO;2

He, J., & Soden, B. J. (2015). Anthropogenic weakening of the tropical circulation: The relative roles of direct co2 forcing and sea surface temperature change. *Journal of Climate*, *28*(22), 8728–8742. doi: https://doi.org/10.1175/JCLI-D-15-0205.1

Held, I. M. (1993). Large-scale dynamics and global warming. *Bulletin of the American Meteorological Society*, *74*(2), 228–242. doi: https://doi.org/10.1175/1520-0477(1993)074⟨0228:LSDAGW⟩2.0.CO;2

Lau, K., Sui, C., & Tao, W. (1993). A preliminary study of the tropical water cycle and its sensitivity to surface warming. *Bulletin of the American Meteorological Society*, *74*(7), 1313–1322. doi: https://doi.org/10.1175/1520-0477(1993)074⟨1313:APSOTT⟩2.0.CO;2

Manabe, S., & Stouffer, R. J. (1980). Sensitivity of a global climate model to an increase of co2 concentration in the atmosphere. *Journal of Geophysical Research: Oceans*, *85*(C10), 5529–5554. doi: https://doi.org/10.1029/JC085iC10p05529

Manabe, S., & Wetherald, R. T. (1975). The effects of doubling the co2 concentration on the climate of a general circulation model. *Journal of the Atmospheric Sciences*, *32*(1), 3–15. doi: https://doi.org/10.1175/1520-0469(1975)032⟨0003:TEODTC⟩2.0.CO;2

Merlis, T. M. (2015). Direct weakening of tropical circulations from masked co2 radiative forcing. *Proceedings of the National Academy of Sciences*, *112*(43), 13167–13171. doi: https://doi.org/10.1073/pnas.1508268112

Moorthi, S., & Suarez, M. J. (1992). Relaxed Arakawa-Schubert. a parameterization of moist convection for general circulation models. *Monthly Weather Review*, *120*(6), 978-1002. doi: https://doi.org/10.1175/1520-0493(1992)120⟨0978:RASAPO⟩2.0.CO;2

Neale, R. B., & Hoskins, B. J. (2000). A standard test for agcms including their physical parametrizations: I: The proposal. *Atmospheric Science Letters*, *1*(2), 101–107. doi: https://doi.org/10.1006/asle.2000.0022

Po-Chedley, S., Armour, K. C., Bitz, C. M., Zelinka, M. D., Santer, B. D., & Fu, Q. (2018). Sources of intermodel spread in the lapse rate and water vapor feedbacks. *Journal of Climate*, *31*(8), 3187-3206. Retrieved from https://doi.org/10.1175/JCLI-D-17-0674.1 doi: 10.1175/JCLI-D-17-0674.1

Po-Chedley, S., Zelinka, M. D., Jeevanjee, N., Thorsen, T. J., & Santer, B. D. (2019). Climatology explains intermodel spread in tropical upper tropospheric cloud and relative humidity response to greenhouse warming. *Geophysical Research Letters*, *46*(22), 13399–13409. doi: https://doi.org/10.1029/2019GL084786

Popke, D., Stevens, B., & Voigt, A. (2013). Climate and climate change in a radiative-convective equilibrium version of echam6. *Journal of Advances in Modeling Earth Systems*, *5*(1), 1–14. doi: https://doi.org/10.1029/2012MS000191

Romps, D. M. (2010). A direct measure of entrainment. *Journal of the Atmospheric Sciences*, *67*(6), 1908–1927. doi: https://doi.org/10.1175/2010JAS3371.1

Romps, D. M. (2011). Response of tropical precipitation to global warming. *Journal of the Atmospheric Sciences*, *68*(1), 123–138. doi: https://doi.org/10.1175/2010JAS3542.1

Romps, D. M. (2014). An analytical model for tropical relative humidity. *Journal of Climate*, *27*(19), 7432–7449. doi: https://doi.org/10.1175/JCLI-D-14-00255.1

Romps, D. M. (2016). Clausius–clapeyron scaling of cape from analytical solutions to rce. *Journal of the Atmospheric Sciences*, *73*(9), 3719–3737. doi: https://doi.org/10.1175/JAS-D-15-0327.1

Santer, B. D., Taylor, K., Wigley, T., Johns, T., Jones, P., Karoly, D., ... others (1996). A search for human influences on the thermal structure of the atmosphere. *Nature*, *382*(6586), 39–46. doi: https://doi.org/10.1038/382039a0

Seeley, J. T., & Romps, D. M. (2015). Why does tropical convective available potential energy (cape) increase with warming? *Geophysical Research Letters*, *42*(23), 10,429-10,437. Retrieved from https://agupubs.onlinelibrary.wiley.com/doi/abs/10.1002/2015GL066199 doi: 10.1002/2015GL066199

Shaw, T. A., Baldwin, M., Barnes, E. A., et al. (2016). Storm track processes and the opposing influences of climate change. *Nature Geoscience*, *9*(9), 656-664. doi: https://doi.org/10.1038/ngeo2783

Sherwood, S. C., Bony, S., & Dufresne, J.-L. (2014). Spread in model climate sensitivity traced to atmospheric convective mixing. *Nature*, *505*(7481), 37–42. doi: https://doi.org/10.1038/nature12829

Singh, M. S., & O'Gorman, P. A. (2013). Influence of entrainment on the thermal stratification in simulations of radiative-convective equilibrium. *Geophysical Research Letters*, *40*(16), 4398-4403. doi: https://doi.org/10.1002/grl.50796

Singh, M. S., Warren, R. A., & Jakob, C. (2019). A steady-state model for the relationship between humidity, instability, and precipitation in the tropics. *Journal of Advances in Modeling Earth Systems*. doi: https://doi.org/10.1029/2019MS001686

Tan, Z., Lachmy, O., & Shaw, T. A. (2019). The sensitivity of the jet stream response to climate change to radiative assumptions. *Journal of Advances in Modeling Earth Systems*, *11*(4), 934–956. doi: https://doi.org/10.1029/2018MS001492

Taylor, K. E., Stouffer, R. J., & Meehl, G. A. (2012). An overview of cmip5 and the experiment design. *Bulletin of the American Meteorological Society*, *93*(4), 485–498. doi: https://doi.org/10.1175/BAMS-D-11-00094.1

Thorne, P. W., Lanzante, J. R., Peterson, T. C., Seidel, D. J., & Shine, K. P. (2011). Tropospheric temperature trends: History of an ongoing controversy. *Wiley Interdisciplinary Reviews: Climate Change*, *2*(1), 66–88. doi:

https://doi.org/10.1002/wcc.80

Tokioka, T., Yamazaki, K., Kitoh, A., & Ose, T. (1988). The equatorial 30-60 day oscillation and the arakawa-schubert penetrative cumulus parameterization. *Journal of the Meteorological Society of Japan. Ser. II*, *66*(6), 883–901. doi: https://doi.org/10.2151/jmsj1965.66.6_883

Tripati, A. K., et al. (2014). Modern and glacial tropical snowlines controlled by sea surface temperature and atmospheric mixing. *Nature Geoscience*, *7*(3), 205. doi: https://doi.org/10.1038/ngeo2082

Vallis, G. K., et al. (2015). Response of the large-scale structure of the atmosphere to global warming. *Quarterly Journal of the Royal Meteorological Society*, *141*(690), 1479-1501. doi: https://doi.org/10.1002/qj.2456

Wang, Y., & Huang, Y. (2020). Understanding the atmospheric temperature adjustment to co2 perturbation at the process level. *Journal of Climate*, *33*(3), 787–803. doi: https://doi.org/10.1175/JCLI-D-19-0032.1

Wing, A. A., Reed, K. A., Satoh, M., Stevens, B., Bony, S., & Ohno, T. (2018). Radiative-convective equilibrium model intercomparison project. *Geoscientific Model Development*, 793–813. doi: https://doi.org/10.5194/gmd-11-793-2018

Supplementary figures for Quantifying the deviation of the tropical upper tropospheric temperature response to surface warming from a moist adiabat

Osamu Miyawaki[1], Zhihong Tan[2], Tiffany Shaw[1], Malte Jansen[1]

[1]Department of the Geophysical Sciences, The University of Chicago
[2]Program in Atmospheric and Oceanic Sciences, Princeton University

Corresponding author: Osamu Miyawaki, miyawaki@uchicago.edu

Table S1. Overprediction in % of the moist adiabat across the model hierarchy for individual models used in this study. Blank data denote models for which data was not available in the corresponding model configuration.

	abrupt4×CO_2	amipF+4×CO_2	amipF	amip4K+4×CO_2	amip4K	aqua4K+4×CO_2	aqua4K
ACCESS1-0	10.6	–	–	–	–	–	–
ACCESS1-3	27.5	–	–	–	–	–	–
bcc-csm1-1	23.1	19.4	15.6	22.8	18.4	–	–
bcc-csm1-1-m	32.3	–	–	–	–	–	–
BNU-ESM	27.1	–	–	–	–	–	–
CanESM2	25.5	15.8	14.0	15.6	13.5	–	–
CCSM4	26.4	22.8	22.9	23.8	23.9	23.6	22.6
CNRM-CM5	46.9	40.3	33.3	40.2	31.9	52.0	40.1
CNRM-CM5-2	46.4	–	–	–	–	–	–
CSIRO-Mk3-6-0	28.0	–	–	–	–	–	–
FGOALS-g2	24.5	–	–	–	–	20.5	17.3
FGOALS-s2	35.5	–	–	–	–	–	–
GFDL-CM3	22.2	–	–	–	–	–	–
GFDL-ESM2G	31.4	–	–	–	–	–	–
GFDL-ESM2M	33.8	–	–	–	–	–	–
GISS-E2-H	23.8	–	–	–	–	–	–
GISS-E2-R	21.2	–	–	–	–	–	–
HadGEM2-ES	12.6	10.0	5.1	11.2	5.6	7.1	4.4
inmcm4	36.6	–	–	–	–	–	–
IPSL-CM5A-LR	27.1	21.0	21.5	21.1	21.7	22.4	23.2
IPSL-CM5A-MR	27.1	–	–	–	–	–	–
IPSL-CM5B-LR	13.4	12.3	12.0	13.1	12.7	–	–
MIROC-ESM	8.2	–	–	–	–	–	–
MIROC5	22.8	17.8	16.0	18.0	15.8	19.4	19.9
MPI-ESM-LR	16.5	16.0	8.3	18.5	9.5	−11.4	−17.3
MPI-ESM-MR	16.9	19.6	11.1	21.3	11.7	−9.3	−15.6
MPI-ESM-P	17.0	–	–	–	–	–	–
MRI-CGCM3	29.8	26.4	23.1	26.5	22.5	24.8	21.1
NorESM1-M	20.9	–	–	–	–	–	–
All model mean	25.3	20.1	16.6	21.1	17.0	16.6	12.9
AMIP-subset mean	23.7	20.1	16.6	21.1	17.0	16.1	12.3
Aqua-subset mean	24.8	21.7	17.6	22.6	17.8	16.6	12.9

Table S2. P-values of the T-test for the null hypothesis that the difference in mean overprediction between the abrupt4×CO_2 response and that of simpler models are indistinguishable. The mean difference and the 5–95% confidence interval are also shown. The difference is statistically significant for all model configurations (p-value < 5%, indicated in bold).

	Lower Bound	Mean	Upper Bound	p-value
abrupt4×CO_2−amipF	4.85	7.10	9.35	**3.58E-5**
abrupt4×CO_2−amip4K	4.01	6.69	9.37	**2.41E-4**
abrupt4×CO_2−aqua4K	2.61	11.96	21.31	**0.0185**

Table S3. Overprediction in % of the moist adiabat across the model hierarchy for various types of the moist adiabat. Three types of moist adiabats are shown here following the definitions in the AMS glossary. *Standard*: The limit of a moist pseudoadiabat when $r_v \ll 1$ (AMS, cited 2020: Moist-adiabatic lapse rate). *Pseudo*: Moist pseudoadiabat, which assumes that all condensates precipitate immediately (AMS, cited 2020: pseudoadiabatic lapse rate). *Reversible*: Reversible moist-adiabat, which assumes that all condensates remain in the rising parcel (AMS, cited 2020: reversible moist-adiabatic process).

	Standard	Pseudo	Reversible
abrupt4×CO_2	25.3	30.5	24.7
amipF	16.6	21.6	15.4
amip4K	17.0	22.1	15.9
aqua4K	12.9	18.6	11.9
GFDLaqua4K	14.2	19.9	13.5
GFDLrce4K	11.6	16.8	11.1

Table S4. P-values of the T-test for the null hypothesis that the difference in mean overprediction averaged over 10°N/S and averaged only over regions of strong mean ascent ($\omega_{500} < -35$ hPa/d, indicated with an asterisk below) are indistinguishable. The mean difference and the 5–95% confidence interval are also shown. The difference is statistically significant for model configurations that have zonally-asymmetric circulations. (p-value < 5%, indicated in bold).

	Lower Bound	Mean	Upper Bound	p-value
abrupt4×CO_2−abrupt4×CO_2^*	3.89	6.10	8.30	**0.0000**
amipF−amipF*	3.92	7.27	10.63	**0.0007**
amip4K−amip4K*	0.88	3.62	6.36	**0.0146**
aqua4K−aqua4K*	−3.76	−0.21	3.35	0.8973

Table S5. P-values of the T-test for the null hypothesis that the difference in mean overprediction between the combined surface warming plus the direct CO_2 response and only the surface warming response are indistinguishable. The mean difference and the 5–95% confidence interval are also shown. The difference is statistically significant for all model configurations (p-value < 5%, indicated in bold).

	Lower Bound	Mean	Upper Bound	p-value
amipF+4×CO_2^*−amipF*	1.53	3.63	5.72	**0.0032**
amip4K+4×CO_2^*−amip4K*	1.54	3.94	6.33	**0.0043**
aqua4K+4×CO_2^*−aqua4K*	0.94	3.15	5.35	**0.0110**

Table S6. Same as Table S3 but overprediction is evaluated only over regions of strong mean ascent ($\omega_{500} < -35$ hPa/d, indicated by an asterisk). This filter is not applied to GFDLrce4K as the RCE configuration lacks a climatological large-scale circulation.

	Standard	Pseudo	Reversible
abrupt4×CO_2^*	19.3	24.6	18.3
amipF*	9.3	14.4	7.7
amip4K*	13.4	18.6	11.9
aqua4K*	13.1	18.8	11.9
GFDLaqua4K*	13.2	18.7	12.4
GFDLrce4K*	–	–	–

Table S7. Same as Table S1 except overprediction is evaluated only over regions of strong mean ascent ($\omega_{500} < -35$ hPa/d, indicated by an asterisk).

	abrupt4×CO_2^*	amipF+4×CO_2^*	amipF*	amip4K+4×CO_2^*	amip4K*	aqua4K+4×CO_2^*	aqua4K*
ACCESS1-0	7.6	–	–	–	–	–	–
ACCESS1-3	23.2	–	–	–	–	–	–
bcc-csm1-1	11.6	5.9	1.4	12.3	7.4	–	–
bcc-csm1-1-m	29.3	–	–	–	–	–	–
BNU-ESM	27.9	–	–	–	–	–	–
CanESM2	10.4	6.2	5.9	9.3	9.1	–	–
CCSM4	29.4	22.2	22.1	26.7	26.6	23.2	21.7
CNRM-CM5	46.2	39.5	32.1	39.8	31.4	50.3	43.0
CNRM-CM5-2	45.5	–	–	–	–	–	–
CSIRO-Mk3-6-0	9.6	–	–	–	–	–	–
FGOALS-g2	22.4	–	–	–	–	19.6	16.9
FGOALS-s2	24.6	–	–	–	–	–	–
GFDL-CM3	18.4	–	–	–	–	–	–
GFDL-ESM2G	30.5	–	–	–	–	–	–
GFDL-ESM2M	31.6	–	–	–	–	–	–
GISS-E2-H	19.8	–	–	–	–	–	–
GISS-E2-R	18.2	–	–	–	–	–	–
HadGEM2-ES	8.1	8.2	4.5	10.7	6.5	5.2	4.7
inmcm4	24.2	–	–	–	–	–	–
IPSL-CM5A-LR	21.0	11.0	8.6	21.5	19.5	21.9	21.8
IPSL-CM5A-MR	19.2	–	–	–	–	–	–
IPSL-CM5B-LR	6.1	11.0	−2.0	3.6	3.4	–	–
MIROC-ESM	−11.3	–	–	–	–	–	–
MIROC5	10.5	10.4	8.3	14.2	11.9	11.0	11.4
MPI-ESM-LR	11.1	9.6	1.8	13.1	4.4	−4.0	−9.9
MPI-ESM-MR	10.0	13.0	4.4	16.2	6.6	−5.4	−10.4
MPI-ESM-P	12.2	–	–	–	–	–	–
MRI-CGCM3	17.9	18.2	15.7	23.4	20.6	24.1	18.6
NorESM1-M	23.2	–	–	–	–	–	–
All model mean	19.2	13.0	9.3	17.3	13.4	16.2	13.1
AMIP-subset mean	16.6	13.0	9.3	17.3	13.4	15.8	12.6
Aqua-subset mean	19.5	16.5	12.2	20.7	15.9	16.2	13.1

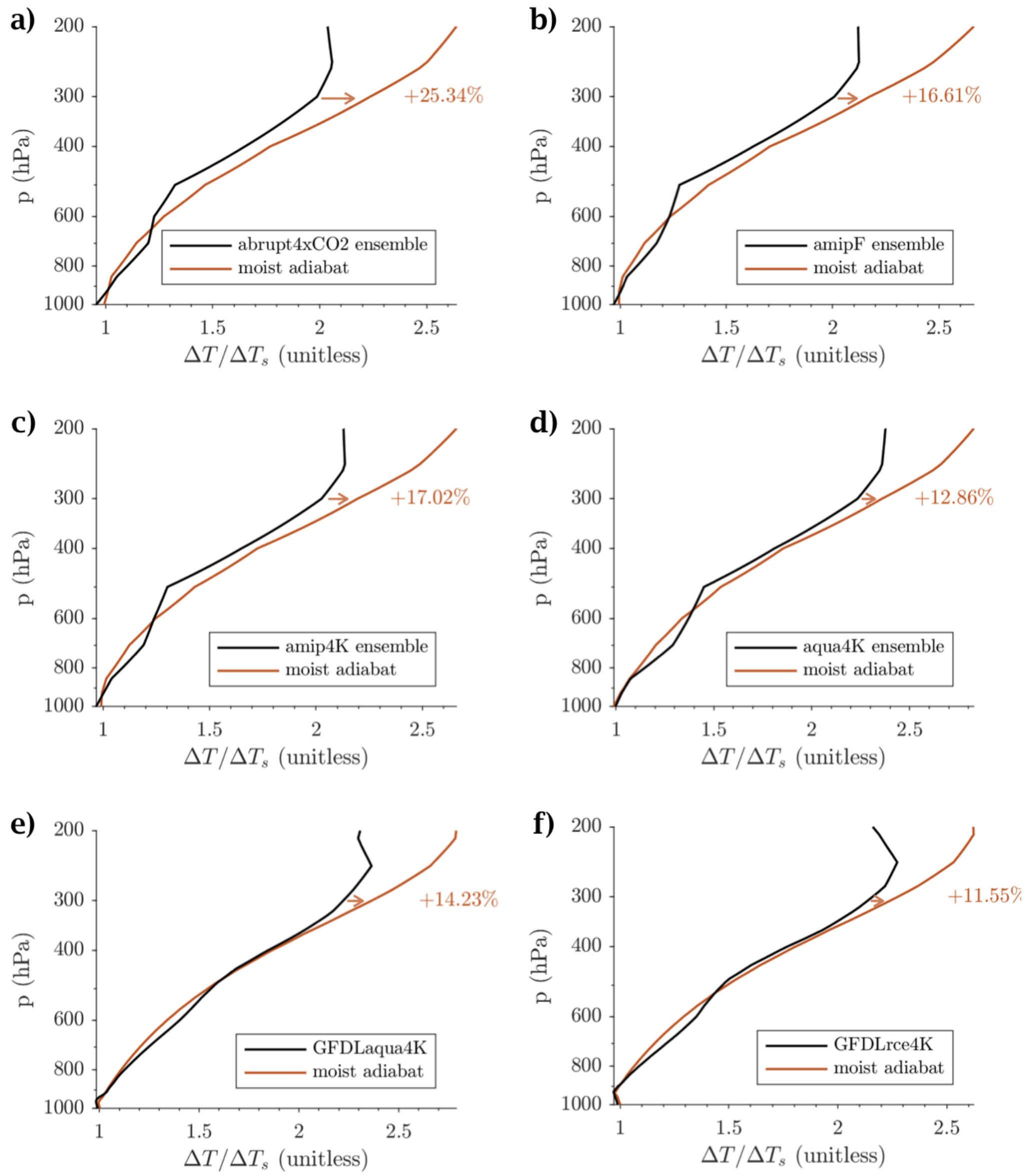

Figure S1. a) Vertical structure of the temperature response over the tropics (defined as 10°N/S) for the CMIP5 multi-model mean (black) and the prediction based on a moist adiabat (orange). The moist adiabat overpredicts the CMIP5 response by 25.34% at 300 hPa. b)–d) are the same for the amipF, amip4K, and aqua4K multi-model mean responses, respectively. e) and f) are the same for GFDLaqua4K and GFDLrce4K responses.

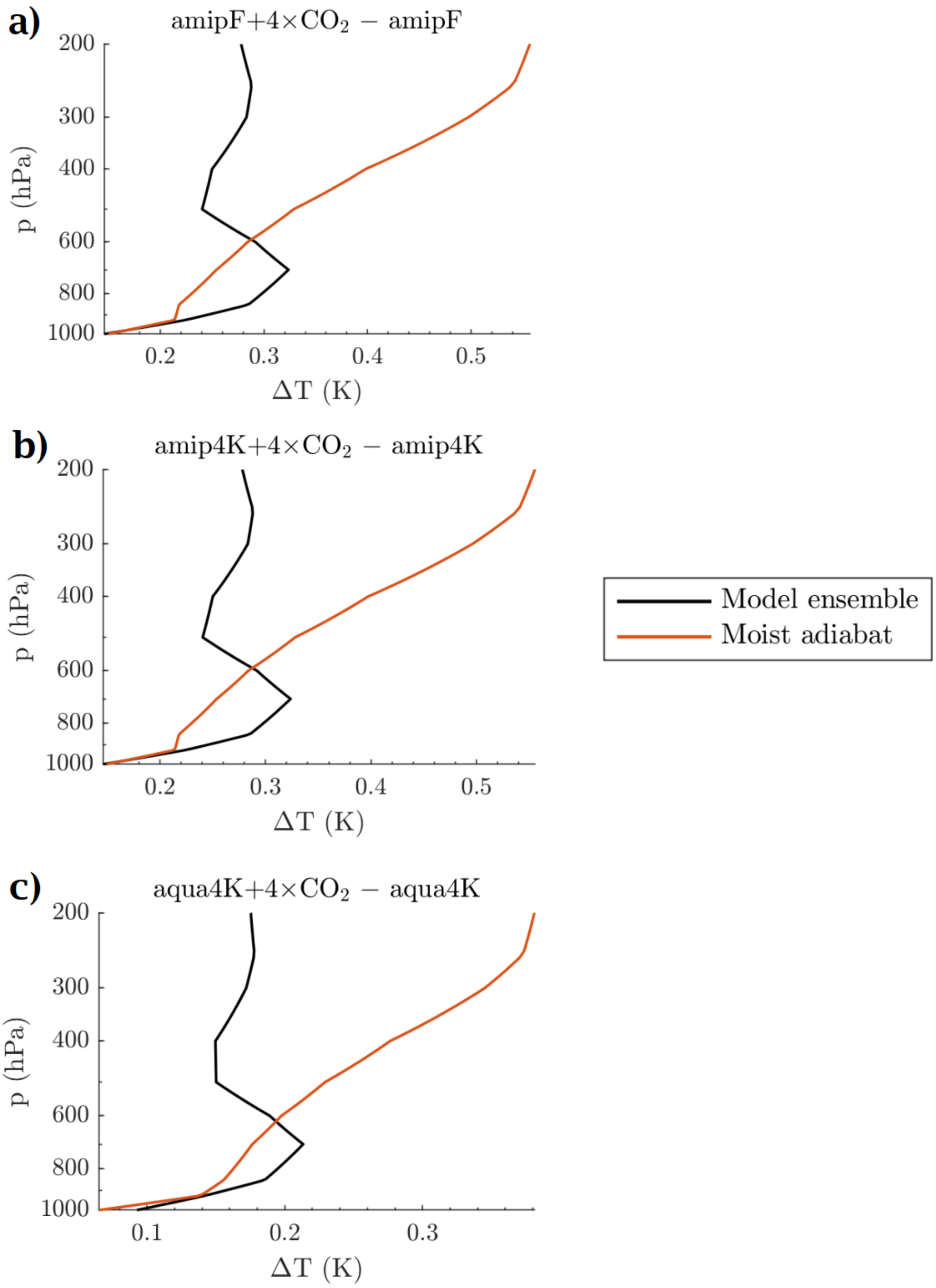

Figure S2. a) Vertical structure of the difference in multi-model mean temperature response between amipF+4×CO_2 and amipF (black) and the corresponding moist adiabatic prediction (orange). While the warming due to the direct effect of CO_2 is approximately uniform with height in the multi-model mean, the moist adiabat predicts amplified warming aloft. b) and c) are the same for the differences between amip4K+4×CO_2 and amip4K and aqua4K+4×CO_2 and aqua4K, respectively.

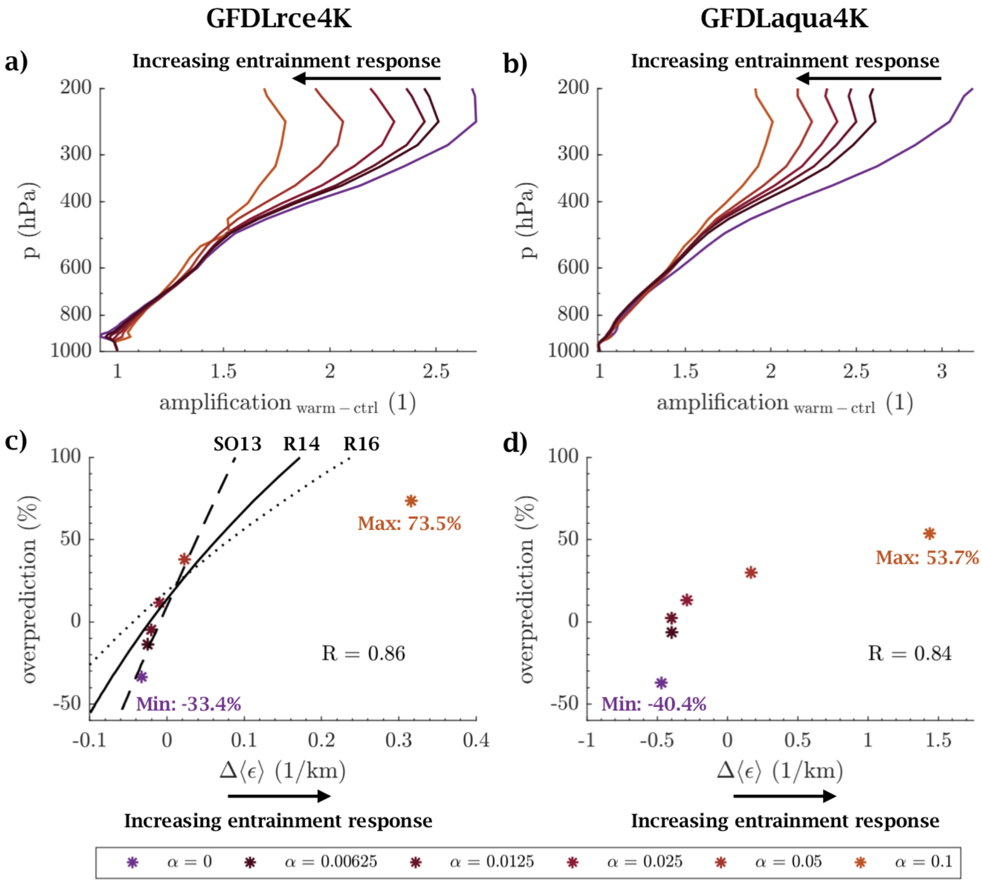

Figure S3. Temperature responses simulated in GFDL where the Tokioka parameter α is held fixed at 0.025 for the control climate and varied as shown only for the warm climate. The amplified warming in the upper troposphere weakens when the entrainment strengthens with warming in a) GFDLrce4K and b) GFDLaqua4K. Overprediction of the moist adiabat scales with the response of entrainment in both c) GFDLrce4K and d) GFDLaqua4K. The deviation as predicted by zero-buoyancy bulk-plume models of Singh and O'Gorman (2013) (labeled SO13), Romps (2014) (R14), and Romps (2016) (R16) are shown as black lines in panel c.

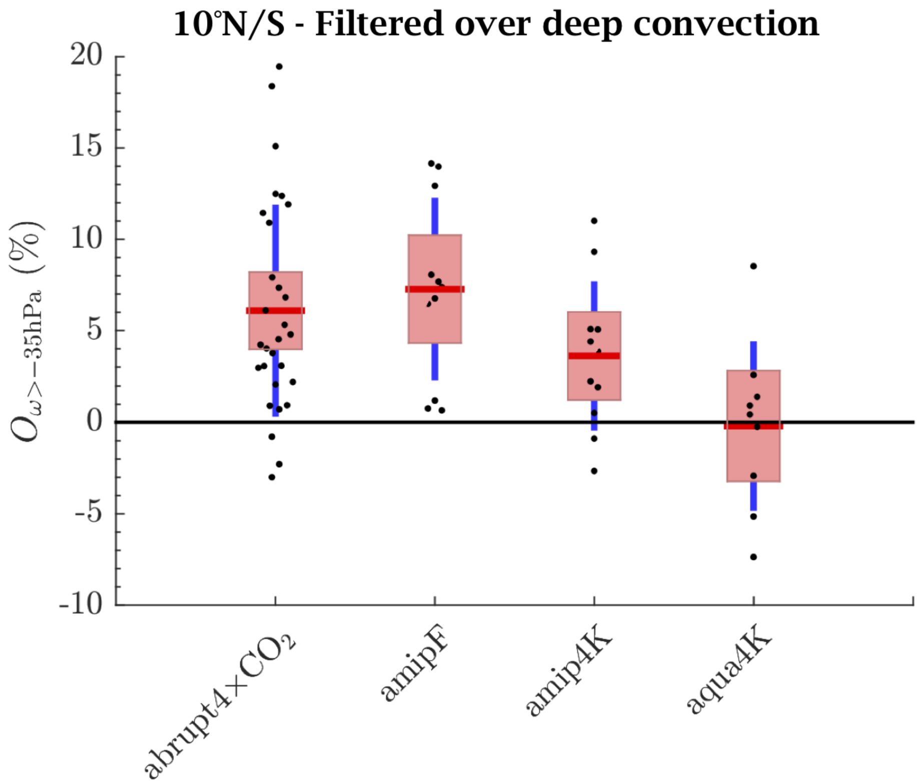

Figure S4. The difference between overprediction averaged over 10°N/S and overprediction averaged only over regions of climatological deep convection ($\omega_{500} < -35$ hPa/d) for each model across the model hierarchy (black dots). The mean difference in overprediction is denoted by the red line. The red box shows the 5–95% confidence interval of the mean. The blue line shows one standard deviation of the distribution.

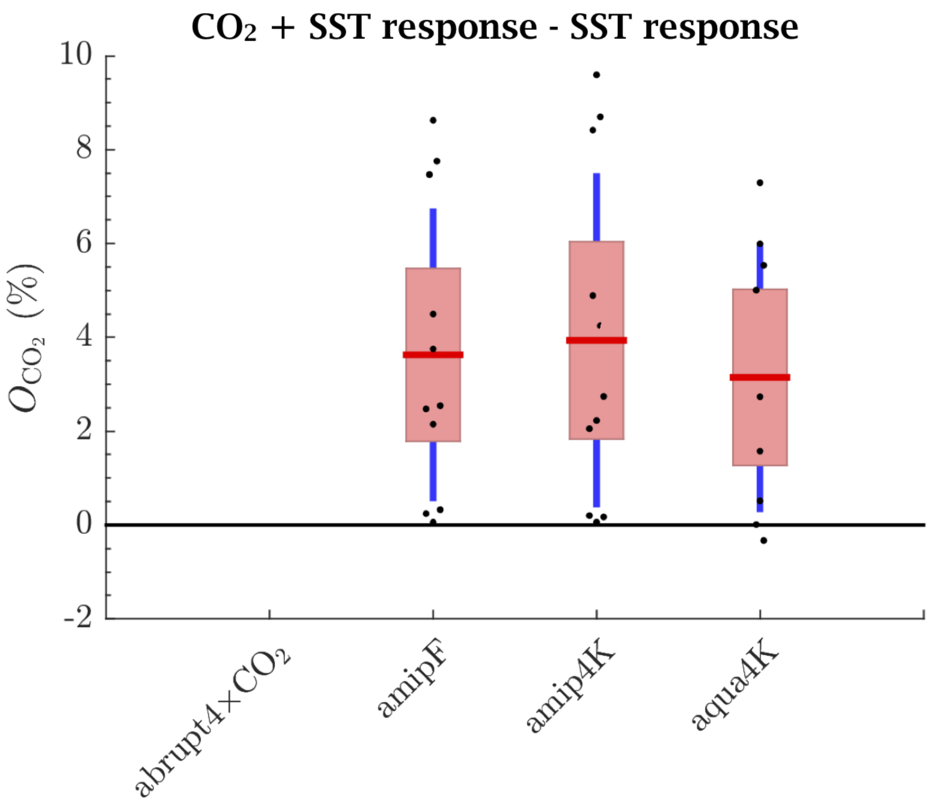

Figure S5. The difference in overprediction between the combined surface warming plus the direct CO_2 response and only the surface warming response for each model across the model hierarchy (black dots). The mean difference in overprediction is denoted by the red line. The red box shows the 5–95% confidence interval of the mean. The blue line shows one standard deviation of the distribution.